PLOS ONE

RESEARCH ARTICLE

Homeodomain-interacting protein kinase (Hipk) plays roles in nervous system and muscle structure and function

Simon J. H. Wang[1,2], Donald A. R. Sinclair[1,3], Hae-Yoon Kim[1,3☯], Stephen D. Kinsey[1,3☯], Byoungjoo Yoo[1,3], Claire R. Y. Shih[1,3], Kenneth K. L. Wong[1,3], Charles Krieger[1,2], Nicholas Harden[1,3], Esther M. Verheyen[1,3]*

1 Centre for Cell Biology, Development and Disease, Simon Fraser University, Burnaby, Canada,
2 Department of Biomedical Physiology and Kinesiology, Simon Fraser University, Burnaby, Canada,
3 Department of Molecular Biology and Biochemistry, Simon Fraser University, Burnaby, Canada

☯ These authors contributed equally to this work.
* everheye@sfu.ca

Citation: Wang SJH, Sinclair DAR, Kim H-Y, Kinsey SD, Yoo B, Shih CRY, et al. (2020) Homeodomain-interacting protein kinase (Hipk) plays roles in nervous system and muscle structure and function. PLoS ONE 15(3): e0221006. https://doi.org/10.1371/journal.pone.0221006

Editor: Efthimios M. C. Skoulakis, Biomedical Sciences Research Center Alexander Fleming, GREECE

Received: July 26, 2019

Accepted: February 13, 2020

Published: March 18, 2020

Data Availability Statement: All relevant data are within the manuscript and its Supporting Information files.

Funding: This work was supported by the Natural Sciences and Engineering Research Council of Canada grants RGPIN/2014-05479, RGPIN/2018-04300, and RGPIN/2018-05964, and the Amyotrophic Lateral Sclerosis Association (CA). The funders had no role in study design, data

Abstract

Homeodomain-interacting protein kinases (Hipks) have been previously associated with cell proliferation and cancer, however, their effects in the nervous system are less well understood. We have used *Drosophila melanogaster* to evaluate the effects of altered Hipk expression on the nervous system and muscle. Using genetic manipulation of Hipk expression we demonstrate that knockdown and over-expression of Hipk produces early adult lethality, possibly due to the effects on the nervous system and muscle involvement. We find that optimal levels of Hipk are critical for the function of dopaminergic neurons and glial cells in the nervous system, as well as muscle. Furthermore, manipulation of Hipk affects the structure of the larval neuromuscular junction (NMJ) by promoting its growth. Hipk regulates the phosphorylation of the synapse-associated cytoskeletal protein Hu-li tai shao (Hts; adducin in mammals) and modulates the expression of two important protein kinases, Calcium-calmodulin protein kinase II (CaMKII) and Partitioning-defective 1 (PAR-1), all of which may alter neuromuscular structure/function and influence lethality. Hipk also modifies the levels of an important nuclear protein, TBPH, the fly orthologue of TAR DNA-binding protein 43 (TDP-43), which may have relevance for understanding motor neuron diseases.

Introduction

Homeodomain-interacting protein kinase (Hipk) family members constitute a group of serine/threonine kinases that phosphorylate many homeodomain transcription factors and influence cell proliferation and tissue growth [1,2]. In *Drosophila*, the single Hipk family member is essential for embryonic and larval survival and when over-expressed, acts as a potent growth regulator that can stimulate tumorigenesis and metastatic cell behavior through its actions on many signaling pathways including Wnt/Wingless, Hippo, Notch and JNK [1,3–8]. In *C. elegans*, the single Hipk ortholog, HPK-1, does not appear to be essential during development, but an *hpk-1* mutant significantly shortens adult lifespan [9]. Vertebrates possess four Hipk

collection and analysis, decision to publish, or preparation of the manuscript.

Competing interests: The authors have declared that no competing interests exist.

orthologs that have some conserved and additional divergent functions (reviewed in [2]). Numerous studies suggest that Hipk family members may also influence signaling pathways related to nervous system development and function. Flies with reduced dHipk possess small eyes with neuronal abnormalities [10,11]. *Hipk-1 Hipk-2* double knockout mice are embryonic lethal and have underdeveloped retinas and defects in neural tube closure [12–14]. Mouse Hipk2 regulates the survival of sensory and sympathetic neurons, and midbrain dopamine neurons [15–17]. In the embryonic midbrain, loss of mouse Hipk2 leads to a decrease in the number of neurons, resulting in Parkinson's disease-like psychomotor abnormalities [17].

The relative level of expression of the *hipk* gene in the nervous system of larvae and adults is robust as described in Flybase [18]. For these reasons, we explored the potential involvement of Hipk in the structure and function of the *Drosophila* nervous system. We show that down-regulation or over-expression of Hipk pan-neuronally, as well as in dopaminergic neurons, glial cells and muscle cells is lethal. However, Hipk mis-expression in motor neurons, cholinergic or glutamatergic neurons has no obvious effects on viability. To investigate the potential causes of lethality from altered expression of Hipk, we focus on larval neuromuscular junctions (NMJs) and muscle and find that Hipk regulates NMJ growth and several synaptic proteins including Hu-li tai shao (Hts; adducin in mammals), Calcium/calmodulin-dependent protein kinase II (CaMKII) and Partitioning-defective 1 (PAR-1; a fly orthologue of microtubule affinity-regulating kinase). These studies demonstrate that Hipk regulates NMJ and muscle organization, and that loss or gain of Hipk negatively affects survival.

Results

Modulation of Hipk in adults leads to premature death

Since it has been shown that a *C. elegans hpk-1* mutant shortens adult lifespan [9], we decided to investigate the role of Hipk in adult *Drosophila* using the Gal4-UAS expression system in combination with a temperature sensitive $Gal80^{ts}$ repressor to over-express and to knock-down Hipk after eclosion. Quantification of knock-down and over-expression efficiency is shown in S1 Fig. We grew flies at 18˚C until adulthood, and then shifted them to 29˚C to inactivate the $Gal80^{ts}$ repressor and to optimize Gal4 transcriptional activation of the UAS constructs. To rule out sex differences we used males in all adult survival analyses. For most studies, we utilized the 17090R-1 RNAi line from the National Institute of Genetics (NIG) to knock down *hipk* gene expression and will refer to this as *UAS-hipk-RNAi*, unless otherwise noted. We first assessed viability of adult males following *hipk* knockdown. The vast majority of *UAS-hipk-RNAi/*$Gal80^{ts}$*; Tub-Gal4/+* males died within 2–4 days after they were shifted from 18˚C to 29˚C (Fig 1A, red curves). With ubiquitous over-expression of Hipk using the HA-tagged *UAS-*$hipk^{3M}$ transgene, (hereafter referred to as *UAS-hipk*), all $Gal80^{ts}$*/+; UAS-hipk/Tub-Gal4* males died within approximately 7–10 days after they were shifted from 18˚C to 29˚C (Fig 1B, red lines). In contrast, identically treated internal control sibling males (Fig 1B, black lines) survived considerably longer. Typically, for both over-expression and knockdown experiments, there was a very small number of experimental flies that escaped early death. In both cases, prior to death, the activity of experimental males slowed progressively until they appeared immobile. These data indicate that both RNAi-induced knockdown and over-expression of Hipk dramatically affects survival and movement of males, suggesting the possibility that the flies may have impaired neuronal, and/or muscle function.

Modulation of Hipk during development affects specific cell types in the nervous system, as well as muscle cells

Based on these observations, we examined developmental effects of Hipk knockdown and over-expression at 29˚C using several nervous system *Gal4* drivers and *Mef2-Gal4*, a muscle-

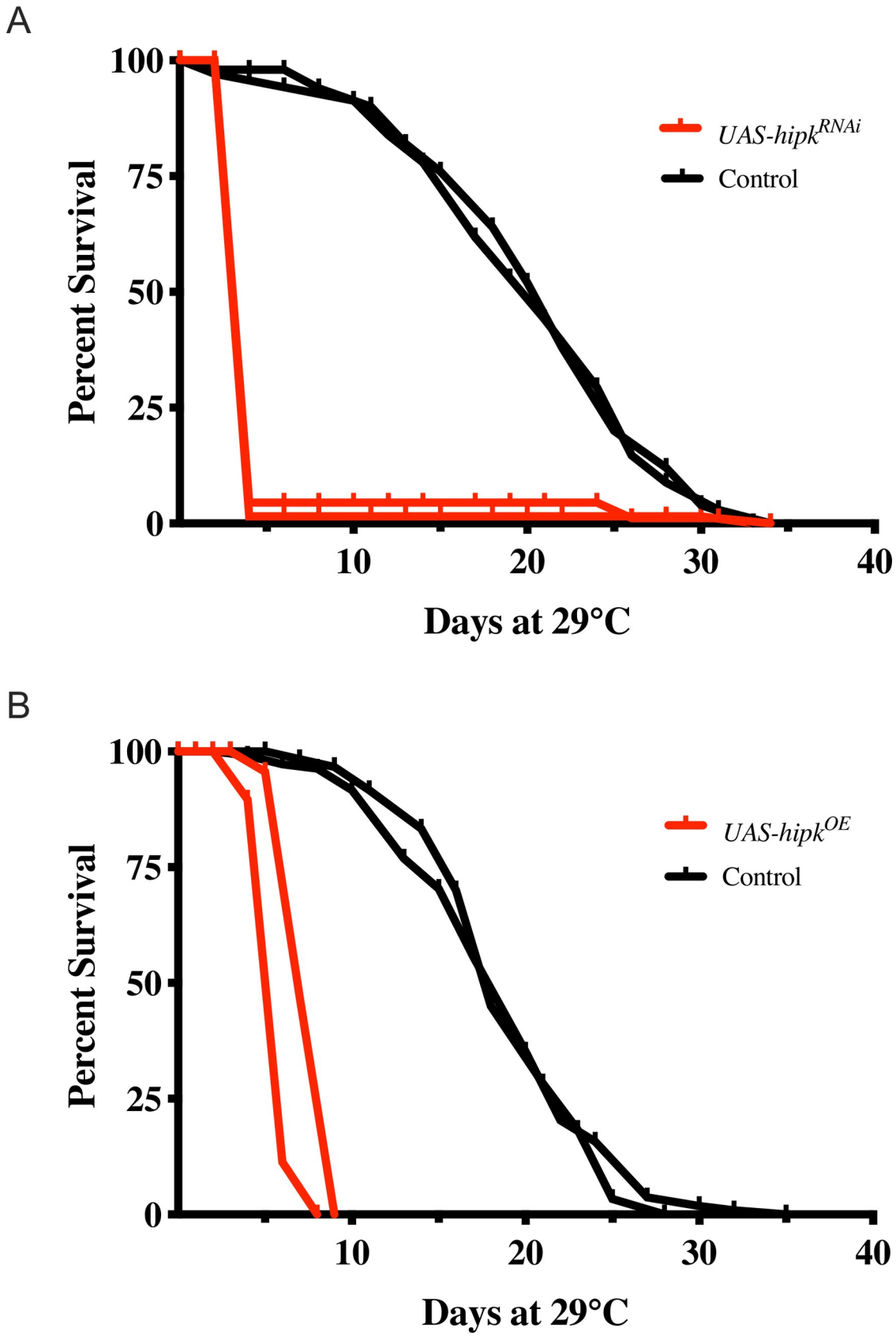
A
100
75
50
25
0
Percent Survival
10
20
30
40
Days at 29°C
UAS-hipk^RNAi
Control
B
100
75
50
25
0
Percent Survival
10
20
30
40
Days at 29°C
UAS-hipk^OE
Control

Fig 1. Ubiquitous modulation of Hipk affects adult life span. (A) Adult males subjected to Hipk knockdown (*UAS-hipk-RNAi/Gal80^{ts}*; *Tub-Gal4*/+; red lines show replicates; n = 89 and n = 65) died within 2 to 4 days at 29˚C. In contrast, internal control male siblings (*TM3*, *Sb*: *UAS-hipk-RNAi/Gal80^{ts}*; *TM3*, *Sb*/+) black lines; n = 69, n = 50) died primarily within 21 to 25 days at 29˚C. (B) Adult males subjected to Hipk over-expression (*UAS-hipk/Gal80^{ts}*; *Tub-Gal4*/+; red lines; n = 69, n = 107) died within 7–10 days at 29˚C. In contrast, internal control males (*Gal80^{ts}*/+; *UAS-hipk/TM3*, *Sb)*; black lines; n = 109 and n = 60) died primarily within 21 to 25 days at 29˚C.

https://doi.org/10.1371/journal.pone.0221006.g001

specific driver (Tables 1 and 2). Pan-neuronal knockdown of Hipk with *Appl-Gal4* resulted in complete lethality with a polyphasic lethal phase. To dissect this effect further we knocked down gene expression in subsets of neurons, namely dopaminergic, cholinergic, glutamatergic and motor neurons. As shown in Table 1, knockdown in dopaminergic neurons using *ple-Gal4* and *TH-Gal4* caused larval/pupal lethality, while knockdown in the other neurons did not affect viability. Knockdown using the pan-neuronal driver *elav-Gal4* resulted in pupal lethality and rare escaping adults had rough eyes (Fig 2B). In addition, it is notable that Hipk knockdown in glial cells was also lethal, with a larval lethal phase. Finally, Hipk knockdown in muscle cells caused lethality at the pupal stage.

To complement the knockdown experiments, we used the same *Gal4* driver strains to assess the effects of over-expression of Hipk during development using *UAS-hipk* (Table 2). We observed lethality at larval and pupal stages upon pan-neuronal expression using *Appl-Gal4*. In contrast, use of *elav-Gal4*, which is expressed in photoreceptors, resulted in rough eyes (Fig 2D). Moreover, Hipk over-expression using *UAS-hipk* in combination with *longGMR-Gal4*, which is expressed in photoreceptor cells, generated flies with an abnormal glassy eye/reduced pigmentation phenotype (Fig 2F). These studies highlight that both gain or loss of Hipk in neurons can affect eye formation and we have previously shown that Hipk is required during larval development for eye specification [10]. Furthermore, as was the case for Hipk knockdown, over-expression in dopaminergic neurons (larval lethal phase, LP), glial cells (larval LP) and muscle cells (larval/pupal LP) was lethal, but over-expression in cholinergic, glutamatergic or motor neurons was not (Table 2).

We extended the developmental analysis in a second set of experiments using a different RNAi transgene *UAS-hipk*-RNAi (V2) and a second Hipk-expressing transgene *UAS-hipk* (attP40) and a subset of nervous system and muscle *Gal4* drivers. The data indicate that, similar to the results for the NIG *hipk*-RNAi transgene, the V2 UAS-*hipk*-RNAi transgene was lethal when expressed in muscles and semi-lethal when expressed throughout the nervous system (S1 Table). However, in contrast to the previous knockdown data, V2 *UAS-hipk-RNAi*-induced

Table 1. Tests for viability of *hipk* knockdown in various nervous system components and muscles using the NIG *UAS-hipk-RNAi*.

***Gal4* Driver**	**Expression**	**% Progeny**		**Total Flies**	**Comments on *UAS-hipk-RNAi***
		UAS-hipk-RNAi	**Control (Balancer)**		
Appl	Pan-neuronal	0	100	100	Polyphasic LP, black structures in ventral termini of pupae
GawB elav^{C155}	Pan-neuronal	16.4	83.6	165	Pupal LP; variably rough eyes with black patches in escaper adults
ple	Dopaminergic	0	100	255	Larval/pupal LP (early pupal death before any body structures are visible)
TH	Dopaminergic	4.3	95.7	115	Larval/pupal LP (early pupal death before any body structures are visible)
ChAT-Gal4.7.4-19B	Cholinergic	54.2	45.8	96	Viable
ChAT-DD.Gal4.VP16	Cholinergic	51.1	48.9	278	Viable
GawB V Glut^{OK371}	Glutamatergic	44.1	55.9	177	Viable
GawB D42	Motor-neuron	50.2	49.8	229	Viable
repo	Glial cells	0	100	155	Larval LP
Mef2	Muscle	0	100	157	Pupal LP (early pupal death before any body structures are visible)

https://doi.org/10.1371/journal.pone.0221006.t001

Table 2. Tests for viability of *hipk* over-expression in various nervous system components and muscles using the 3M *UAS-HA-hipk*.

Gal4 Driver	Expression	% Progeny		Total Flies	Comments on *UAS-hipk*
		UAS-HA-hipk	Control (Balancer)		
Appl	Pan-neuronal	0.9	99.1	106	Larval/pupal LP
GawB elav^{C155}	Pan-neuronal	26.9	73.1	67	Rough eyes
ple	Dopaminergic	0	100	225	Polyphasic LP, some early pupal death before any body structures are visible, black pupae
TH	Dopaminergic	0	100	158	Larval/pupal LP (early pupal death before any body structures are visible)
ChAT-Gal4.7.4-19B	Cholinergic	55.5	44.5	164	Viable
ChAT-DD.Gal4. VP16	Cholinergic	51.1	48.9	278	Viable
GawB V Glut^{OK371}	Glutamatergic	54.3	45.7	175	Viable
GawB D42	Motor-neuron	40.1	59.9	142	Viable
repo	Glial cells	0	100	174	Larval LP
Mef2	Muscle	0	100	156	Larval/pupal LP (early pupal death before any body structures are visible)

https://doi.org/10.1371/journal.pone.0221006.t002

knockdown in dopaminergic neurons as well as in glial cells, had no effect. In addition, in agreement with the previous over-expression data, the attP40 *UAS-hipk* transgene is lethal/semi-lethal when expressed throughout the nervous system and semi-lethal when expressed in dopaminergic neurons (S2 Table). However, in contrast to the previous overexpression data, expression of the attP40 *UAS-hipk* transgene in muscles and glial cells had no effect. We believe that the aforementioned differences in the data are due to variable potency of the V2 *UAS-hipk*-RNAi and attP40 *UAS-hipk* transgenes (S1 Fig). Collectively, our data suggest that Hipk regulates elements of the fly nervous system and that Hipk causes lethality when mis-expressed in a subset of neurons and glial cells. In addition, the lethal effects of perturbation of Hipk in muscle indicate essential roles in the development and/or function of the tissue.

Hipk is present in the muscle cytoplasm and nuclei during larval NMJ development, and regulates NMJ size

As modulation of Hipk levels with *Mef2-Gal4* caused pupal lethality, we examined the distribution of Hipk at the neuromuscular junction (NMJ) of 3rd instar larvae. In wild-type, Hipk immunoreactivity was observed as punctate labeling throughout the muscle cytoplasm and within the DAPI-negative regions of muscle nuclei, with no obvious accumulations at the NMJ (Fig 3A–3A‴ and 3C–3C″). Muscle-specific Hipk over-expression led to increased Hipk extra-synaptic puncta (Fig 3B–3B‴‘). Most strikingly, however, muscle nuclei displayed considerable Hipk immunoreactivity in the form of large, round bodies that consisted of strong Hipk labeling at the surface of these structures with an internal core area containing less Hipk labeling (Fig 3B'–3B‴ and 3D–3D″). These structures were present in the DAPI-negative regions of the nucleus but did not localize within the nucleolus.

Given the presence of Hipk during larval NMJ development, we next tested for Hipk-mediated effects on NMJ size. Hipk over-expression in the muscle led to a 1.2-fold increase in NMJ surface area, in comparison to the wild-type control (Fig 3A and 3B; quantifications in S2A Fig; see Fig 3E for normalized data). Interestingly, the number and size of muscle nuclei also increased with Hipk over-expression (S2B and S2C Fig). In contrast, measurements of muscle surface area showed a 1.2-fold decrease for Hipk over-expressing tissue (S2D Fig). This result suggests that Hipk can also modulate muscle growth, and that the reduced muscle size contributes to the increased ratio observed between NMJ and muscle surface area to an equal or

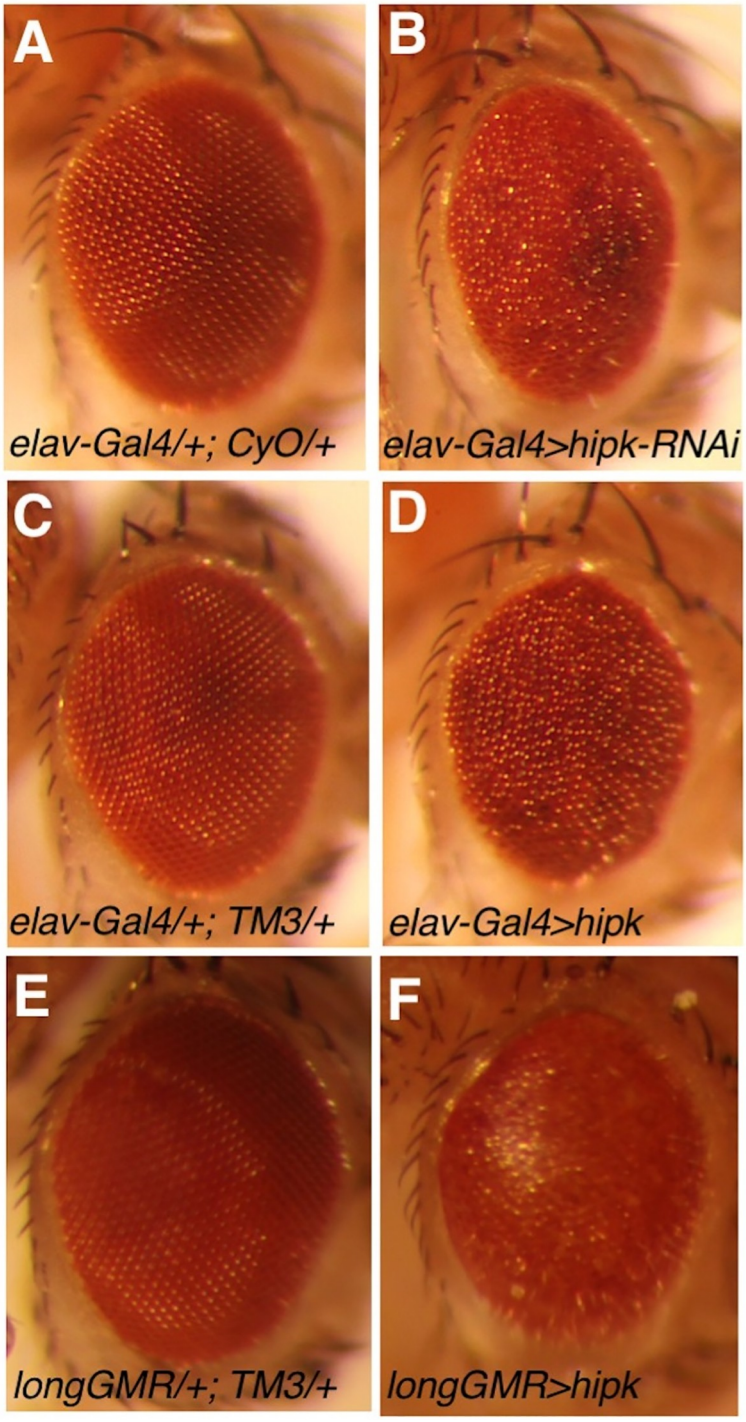

Fig 2. Disrupted eye patterning due to modulation of Hipk at 29˚C. The eyes of internal control females (A: *elav-Gal4*/+; *CyO*/+; C: *elav-Gal4*/+; *TM3*, *Sb*/+; E: *longGMR-Gal4*/+; *TM3*, *Sb*/+) are normal. In contrast, the eyes of (B) *elav-Gal4*/+; *UAS-hipk-RNAi*/+ and (D) *elav-Gal4*/+; *UAS-hipk*/+ females are rough, whereas those of (F) *longGMR-Gal4*/+; *UAS-hipk*/+ females are smooth and have somewhat reduced pigmentation.

https://doi.org/10.1371/journal.pone.0221006.g002

greater degree than the increased NMJ growth (see Fig 3E for normalized data). Expression of transgenic *hipk-RNAi* in the muscle caused severe NMJ and muscle morphological defects

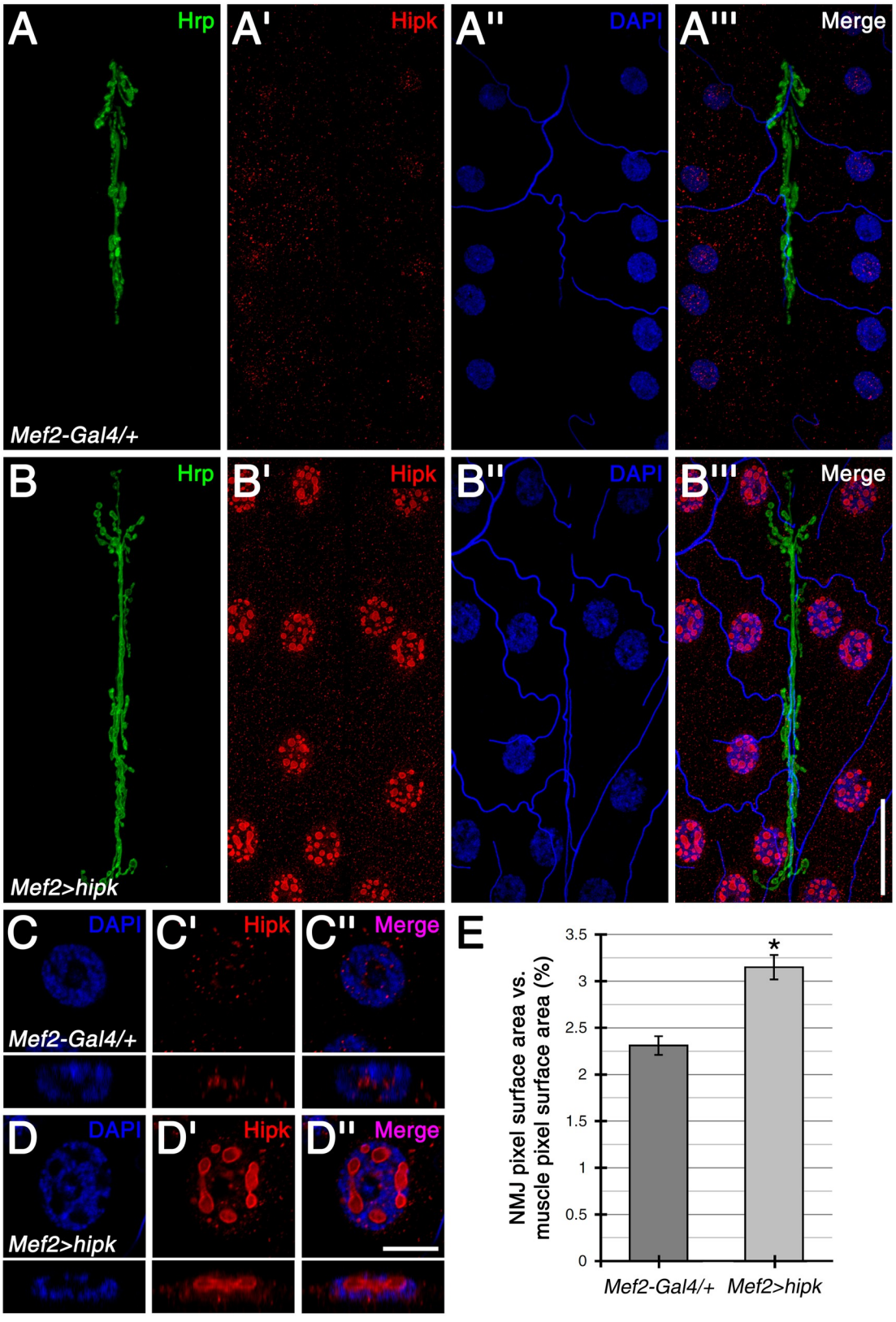

Fig 3. Hipk is present throughout the muscle cytoplasm and within muscle nuclei during larval NMJ development. (A-A"') In wild-type control (i.e. *Mef2-Gal4* outcrossed to w^{1118}) larval body wall muscles, Hipk showed an extra-synaptic punctate

distribution throughout the muscle cytoplasm and within muscle nuclei, which were marked with DAPI. No distinct accumulations were observed at the NMJ, which was marked by Hrp. (B-B"') Muscle-specific expression of *UAS-hipk* with *Mef2-Gal4* (*Mef2-Gal4>hipk*) led to increased Hipk puncta in the muscle cytoplasm. Most strikingly, Hipk also accumulated within muscle nuclei as large, round bodies. (C-D") Magnified, single-sectional views of muscle nuclei. For the wild-type control, Hipk puncta were found within the nucleus, primarily in DAPI-negative regions (C-C", see cross-sectional views in the panels directly below). With Hipk over-expression in the muscle, Hipk was present at both the boundary and within the nuclear bodies, which were also localized in DAPI-negative regions (D-D", see cross-sectional views). (E) Quantification of the effects of Hipk on NMJ size. NMJ size was measured as NMJ pixel surface area normalized against muscle pixel surface area (%). Over-expression of Hipk in the muscle resulted in significantly larger NMJs (a 1.4-fold increase) when compared to the wild-type control. Sample size was 24 NMJs from 12 body walls for each genotype. * $p<0.0001$. Scale bars: 40μm (A-B"'); 10uM (C-D").

https://doi.org/10.1371/journal.pone.0221006.g003

(S3B Fig) and was not analyzed further in this study. As Hipk did not specifically localize to either the pre- or post-synapse of the NMJ at endogenous or over-expressed levels, Hipk regulation of NMJ size likely arises from indirect modulation of synaptic proteins.

Hipk regulates multiple post-synaptic proteins, including the cytoskeletal protein, Hts

To elucidate Hipk's role in regulating NMJ size in the muscle, we assessed the distribution of multiple post-synaptic proteins in Hipk over-expressing larvae. No effects on the synaptic levels of Glutamate receptor IIA (GluRIIA) were observed between muscle-specific Hipk over-expression and the wild-type control (S4A Fig). However, over-expression of Hipk resulted in significantly lower α-Spectrin (α-Spec) levels (S4B Fig) but higher Fasciclin 2 (Fas2) levels (S4C Fig) at the NMJ. As the mode of regulation differed between the post-synaptic proteins evaluated, the observed alterations associated with Hipk over-expression appear to be specific, and not due to artificial or non-specific causes.

Another post-synaptic protein that has been shown to regulate NMJ growth is the actin-spectrin associated protein, adducin/Hts [19,20]. In wild-type control NMJs, Hts predominately localized to the postsynaptic membrane (Fig 4A–4A"). Hts was also present extra-synaptically throughout the muscle membrane as punctate structures organized in a lattice-like pattern (observed in 8 out of 8 muscle 6/7 pairs evaluated) (Fig 4E), a distribution that is found with spectrin networks in other systems [21,22]. Muscle-specific over-expression of Hipk resulted in slightly higher levels of Hts at the NMJ (Fig 4B–4B"; see S5A Fig for quantification). However, Hts distribution throughout the extra-synaptic muscle membrane was largely undetectable or disrupted (observed in 8 out of 8 muscle 6/7 pairs) (Fig 4F). In addition, aberrant accumulations of Hts often formed in some regions of the muscle cytoplasm (observed in 7 out of 8 muscle 6/7 pairs; never observed in the wild-type control) (Fig 4G). These results indicate that Hipk negatively regulates Hts extra-synaptic distribution at the muscle membrane.

In many cell types, phosphorylation of adducin/Hts by protein kinase C (PKC) or cAMP-dependent protein kinase (PKA) can inhibit the interactions of adducin/Hts with the spectrin-actin cytoskeleton, and cause adducin/Hts to redistribute from the plasma membrane to the cytoplasm [23]. To determine if Hipk affects Hts distribution at the muscle membrane through modulating Hts phosphorylation levels, we used an antibody that detects phosphorylation of the mammalian adducins at the PKC/PKA target site in the myristoylated alanine-rich C-kinase (MARCKS) domain. The site is conserved in *Drosophila* Hts, and the antibody has been previously used on larval muscles to detect Hts phosphorylation [24]. In the wild-type control, Hts phosphorylation was observed at the NMJ, and was also present as puncta that formed the lattice-like network in the muscle described above (observed in 8 out of 8 muscle 6/7 pairs evaluated) (Fig 4C–4C" and 4H). Muscle-specific over-expression of Hipk suppressed Hts phosphorylation, as lower levels of p-adducin immunoreactivity were observed at the NMJ (Fig 4D–4D"; see S5B Fig for quantification), and the lattice-like network in the muscle was

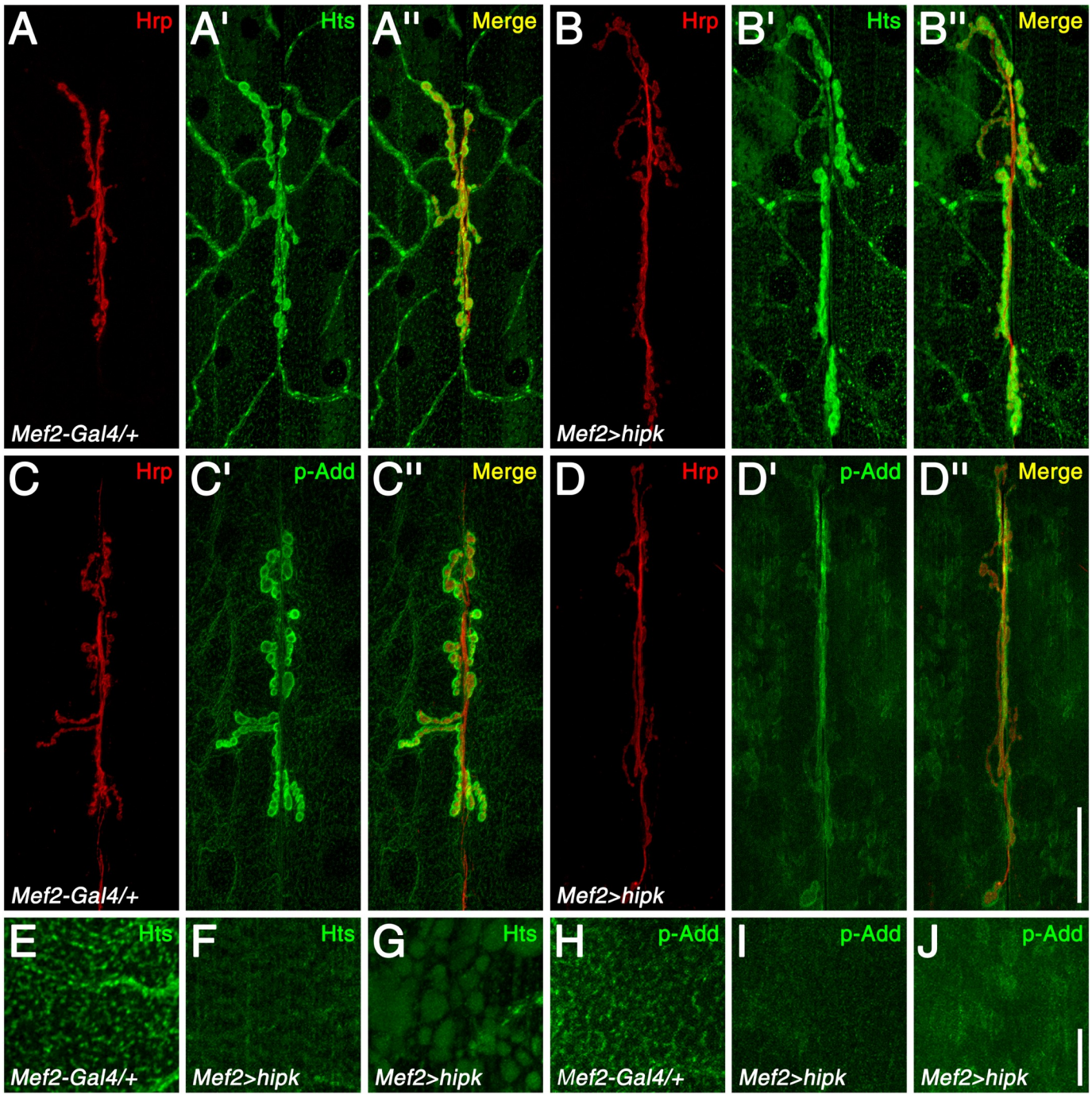

Fig 4. Hipk disrupts Hts distribution in the muscle and suppresses its phosphorylation at the MARCKS domain. (A-A") In control tissue (*Mef2-Gal4/+*), Hts localized to the NMJ. In addition, Hts puncta formed a lattice-like network throughout the muscle. (B-B") With Hipk over-expression in the muscle (*Mef2-Gal4>hipk*), Hts still localized to the post-synaptic membrane of the NMJ. However, the organization of the Hts muscle puncta was disrupted. Cloudy accumulations in the muscle were also often observed. (C-C") p-Add immunoreactivity in the wild-type control was present at the NMJ and was also observed as puncta that formed the lattice-like network in the muscle. The antibody detects an Add phosphorylation site in the MARCKS domain, which is conserved in Hts. (D-D") Muscle-specific over-expression of Hipk reduced p-Add immunoreactivity, as lower signal levels were observed at the NMJ, and the lattice-like network in the muscle was missing. In addition, aberrant accumulations were observed in the cytoplasm. (E-J) High-magnification views of Hts and p-Add immunoreactivity in a section of muscle membrane, showing the lattice-like network in wild-type (E and H) and Hipk over-expression phenotypes, *i.e.* disrupted organization (F and I) and aberrant accumulations (G and J). Scale bars: 40μm (A-D"); 10μm (E-J).

https://doi.org/10.1371/journal.pone.0221006.g004

missing (observed in 8 out of 8 muscle 6/7 pairs) (Fig 4I). In addition, aberrant accumulations in regions of the muscle cytoplasm were sometimes present (observed in 4 out of 8 muscle 6/7 pairs; never observed in the wild-type control) (Fig 4J). These results indicate that Hipk influences the phosphorylation of Hts, either directly or indirectly.

Hipk suppresses CaMKII and PAR-1 expression, thus modulating Dlg phosphorylation

We have previously shown that Hts regulates the post-synaptic localization of the important scaffolding molecule, Discs large (Dlg), by elevating the levels of the kinases, CaMKII and PAR-1, in the muscle [20]. CaMKII and PAR-1 phosphorylate Dlg at the PDZ1 and GUK domains, respectively, which disrupts Dlg postsynaptic targeting [25,26] and influences synaptic stability [27]. To assess if Hipk modulates this function of Hts, CaMKII and PAR-1 immunoreactivity were observed in the muscles of control and Hipk over-expressing larvae. CaMKII and PAR-1 typically localize to the NMJ, but are also present throughout the muscle (Fig 5A and 5C), as shown previously [25,26]. When Hipk was over-expressed in the muscle, immunoreactivity against CaMKII and PAR-1 appeared to be reduced (Fig 5B and 5D). PAR-1 immunoreactivity at the muscle membrane was missing in comparison to the wild-type control (compare corresponding cross-sections for Fig 5D and 5C). CaMKII immunoreactivity at the muscle membrane was also missing, revealing the underlying striated pattern of the sarcomeres (compare cross-sections for Fig 5B and 5A). To confirm the observed decreases in CaMKII and PAR-1 immunoreactivity, and to determine if the alterations were due to changes at the transcript level, FISH was performed with the use of labeled antisense probes that bind to *camkII* and *par-1* mRNA. Endogenous *camkII* and *par-1* transcripts appeared as puncta throughout the muscle cytoplasm, with prominent accumulations found within muscle nuclei (Fig 5E–5E" and 5G–5G") [24]. However, muscle-specific Hipk over-expression caused overall reductions in the levels of both transcripts (Fig 5F–5F" and 5H–5"H; quantifications in S6A and S6B Fig). These results indicate that Hipk suppresses the expression of CaMKII and PAR-1 at the transcript level, thereby modifying the levels and distribution of these kinases in the muscle.

We next assessed Hipk-mediated effects on Dlg phosphorylation. To accomplish this, we made use of an antibody that specifically detects Dlg phosphorylation at the PAR-1 target site [26]. With this antibody, Dlg phosphorylation is undetectable in *par-1* mutant larval body wall muscle extracts via Western blot analysis (Zhang et al., 2007b). Unfortunately, no antibody against phosphorylation at the CaMKII target site was available, thus we were unable to test this directly. In the wild-type control, p-Dlg^{S797} immunoreactivity was observed at the NMJ and as puncta throughout the muscle cytoplasm (Fig 5I), as previously reported [20,26]. However, when Hipk was over-expressed in the muscle, extra-synaptic p-Dlg puncta levels were significantly decreased (Fig 5J; quantification in S6C Fig). Collectively, our data indicate that Hipk can modulate the phosphorylation of Dlg by PAR-1, and likely CaMKII as well, through negatively regulating the expression of these kinases.

Hipk can modulate TBPH levels

Nuclear Hipk proteins have been previously associated with nuclear structures known as 'Hipk domains' [28], PML bodies, or paraspeckles [29]. To further investigate the relationship between the striking nuclear Hipk structures observed with Hipk over-expression and that of other nuclear factors, we performed immunocytochemistry with antibodies to two nuclear proteins demonstrated to have extensive roles in the nervous system. For instance, TAR DNA-binding protein 43 (TDP-43) is a DNA- and RNA-binding protein predominantly localized to

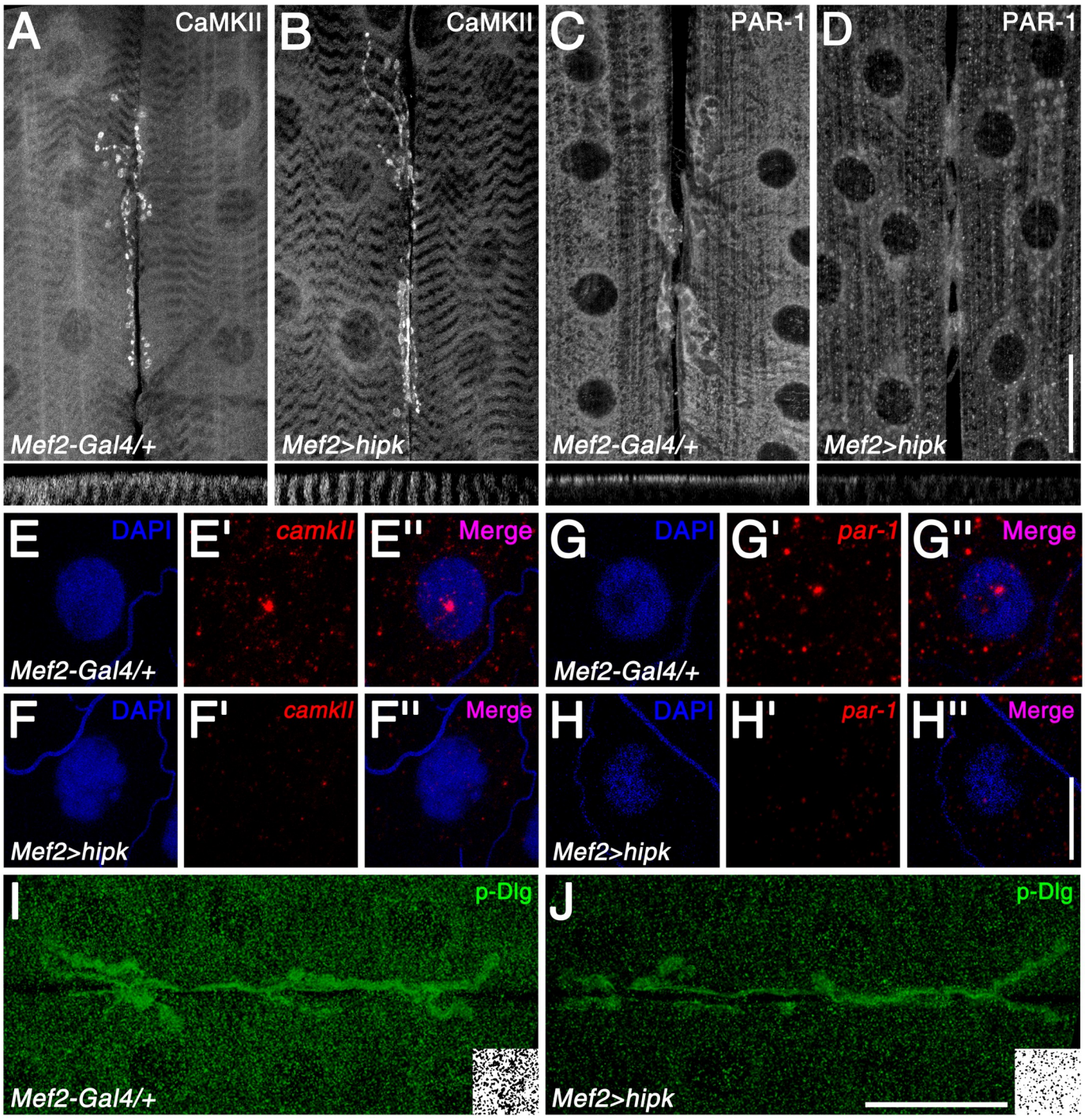

Fig 5. Hipk reduces Dlg phosphorylation through negative regulation of PAR-1, and most likely CaMKII, expression. (A) In the control (*Mef2-Gal4/+*), CaMKII localized specifically at the NMJ, but was also present throughout the muscle cytoplasmic surface (see cross-section of the muscle in the panel directly below). (B) Muscle-specific Hipk over-expression (*Mef2-Gal4>hipk*) led to reduced CaMKII levels in the muscle, exposing the underlying striated pattern of the sarcomeres (more easily observed in the cross-section). (C) Similar to CaMKII, PAR-1 in the wild-type control was present at the NMJ and muscle cytoplasmic surface (see cross-section). (D) Hipk over-expression also resulted in lower PAR-1 levels in the muscle (more easily observed in the cross-section). (E-E") In the wild-type control, *camkII* transcripts were found as distinct accumulations within muscle nuclei, with lower levels of puncta found in the muscle cytoplasm. DAPI was used to mark the nuclei. (F-F") Over-expression of Hipk in the muscle caused a marked decrease in overall *camkII* transcript levels. (G-H") Similar results were observed for *par-1* transcripts. (I) p-Dlg in the wild-type control was observed at the NMJ and as puncta throughout the muscle cytoplasm. The antibody detects Dlg phosphorylation at the PAR-1 target site in the GUK domain. Inset shows p-Dlg immunoreactivity in a section of muscle that was converted to a black-and-white image. (J) Hipk over-expression resulted in reduced p-Dlg puncta levels in the muscle (compare insets). Scale bars: 40μm (A-D); 20μm (E-H"); 40μm (I, J).

https://doi.org/10.1371/journal.pone.0221006.g005

the nucleus that has roles in transcriptional regulation, as well as RNA processing and stability [30,31]. This protein is present in *Drosophila*, where it has been well characterized and is called TBPH [30]. Additionally, fused in sarcoma (FUS/TLS), which in *Drosophila* is represented by Cabeza (Caz, or dFUS), is a nuclear-associated transcriptional activator which has also been well characterized [32]. Mutations in TDP-43 and FUS have been identified in patients with the familial form of the neurodegenerative disorder amyotrophic lateral sclerosis (ALS), which is characterized by progressive loss of motoneurons and muscle atrophy.

In the wild-type control, Caz localized predominately to muscle nuclei (Fig 6A). Muscle-specific Hipk over-expression did not alter Caz distribution or levels (Fig 6B; see S7A Fig for quantification). TBPH immunoreactivity in the wild-type control showed a largely nuclear distribution, with some labeling in the muscle and axon (Fig 6C). In contrast, with Hipk over-expression, TBPH immunoreactivity was strikingly reduced in the nucleus (Fig 6D; see S7B Fig for quantification). Nuclear loss or clearance of TDP-43/TBPH is seen in a variety of neurological disorders including ALS, as well as fly models of ALS [30,33].

A deleterious interaction between Hipk over-expression and TBPH over-expression was seen when Hipk (using attP40 *UAS-hipk*, which itself does not cause an eye phenotype when driven with *longGMR-Gal4* (Fig 6E)) was co-expressed with *UAS-TBPH* in *Drosophila* eyes, using *longGMR-Gal4*, leading to a rough/necrotic eye phenotype (Fig 6I). On the other hand, analogous co-expression of *UAS-caz* had no striking effect (Fig 6G).

Discussion

Previous work has shown that elevated expression of Hipk leads to tumorigenesis and metastatic cell behavior, likely by stimulating various signaling pathways such as Wnt/Wingless, Hippo, Notch and JNK [3,4,6–8,34]. However, relatively little is known regarding the action of Hipk in the nervous system and muscle. We find that ubiquitous over-expression and knockdown of Hipk have dramatic effects on adult survival leading to progressive immobility and death, and these effects are most likely due to perturbations in the nervous system and muscle. Evidence for nervous system involvement during development is supported by the observation of rough eye phenotypes associated with pan-neuronal and/or eye-specific Hipk knockdown and over-expression, as well as by the fact that such mis-expression in dopaminergic neurons and glial cells is lethal. Taken together, these results show that both reduced and excessive levels of Hipk have profound effects on nervous system function in flies. Our adult-specific data are consistent with observations that *Hipk2* knockout mice exhibit increased perinatal lethality and that a mutation in the *C. elegans* ortholog, *hpk-1*, shortens lifespan [9,35]. The effects of Hipk misexpression in dopaminergic neurons is of significant interest since these neurons are affected by human neurodegenerative disorders such as Parkinson's disease. Such effects are consistent with the previously mentioned role of mammalian Hipk2 in survival of midbrain dopaminergic neurons [17].

Distribution of Hipk during larval NMJ development

Our results demonstrate that Hipk is present in muscle nuclei where Hipk likely phosphorylates transcription factors and other substrates. Interestingly, we have also found that muscle-specific knockdown in *Drosophila* adults dramatically shortens their lifespan and that death is preceded by progressive immobility supporting our claim that muscle and neuronal function are regulated by Hipk. Under control conditions Hipk is predominantly intranuclear where it is found in small puncta, as described previously [8]. As previous work did not clearly localize these puncta to identified subnuclear structures they have been referred to as 'Hipk domains' [28]. In some cases, Hipk localization has been associated with the subnuclear promyelocytic

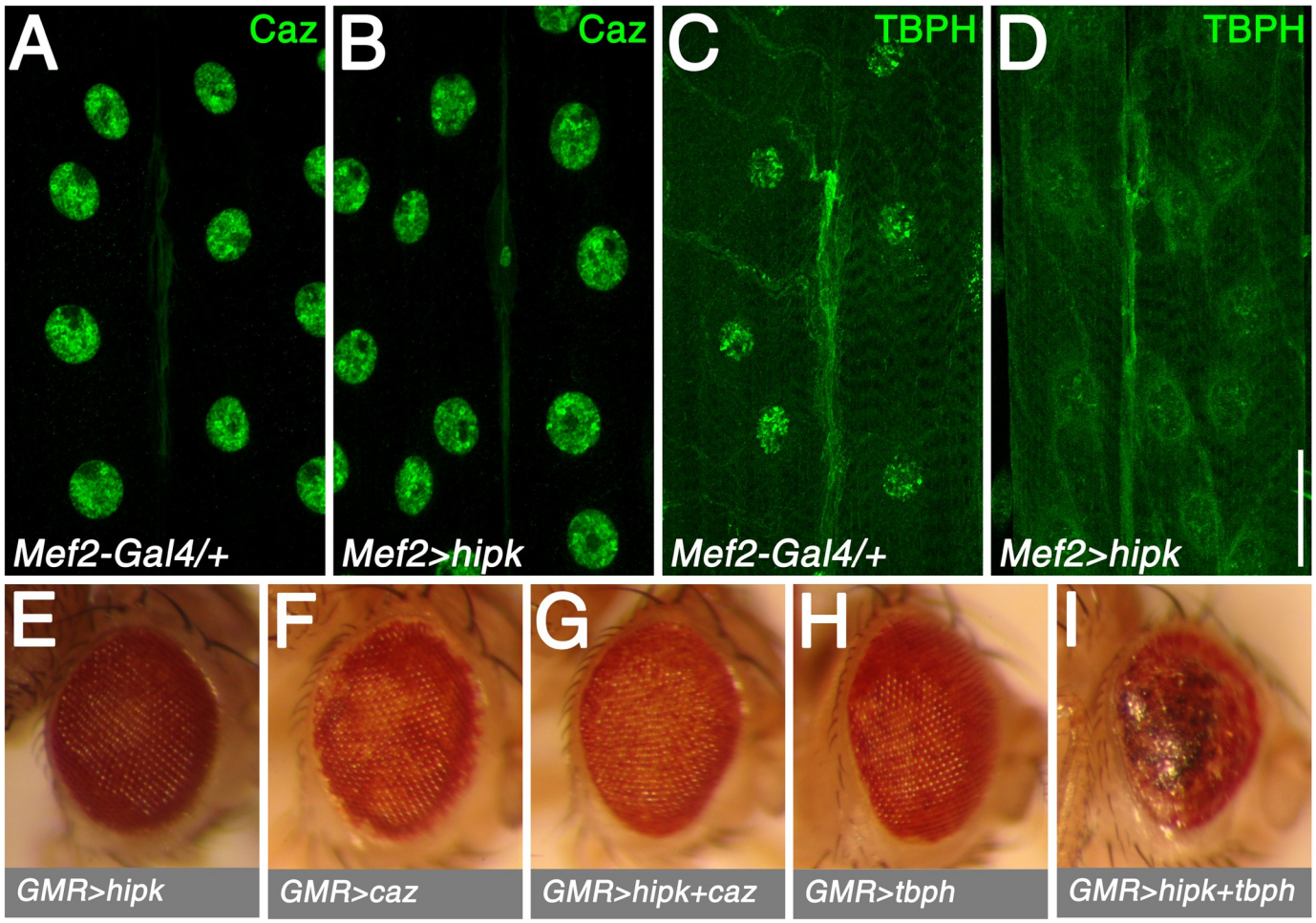

Fig 6. Hipk has distinct effects on the ALS-associated proteins, FUS/Caz and TDP-43/TBPH. (A) In control tissue (*Mef2-Gal4/+)*, Caz localized predominately to muscle nuclei. (B) Muscle-specific over-expression of Hipk (*Mef2-Gal4>hipk*) caused no observable effects on Caz distribution or levels. (C) TBPH was also most prevalent in muscle nuclei in the control. (D) Hipk over-expression in the muscle resulted in reduced nuclear TBPH levels. (E-I) Genotypes for eye images (all males incubated at 29˚C): *UAS-hipk/+; longGMR-Gal4/+* (E), *UAS-caz/CyO; longGMR-Gal4/+* (F), *UAS-hipk/UAS-caz; longGMR-Gal4/+* (G); *CyO/ UAS-TBPH; longGMR-Gal4/+* (H), and *UAS-hipk/UAS-TBPH; longGMR-Gal4/+* (I). Scale bar: 40μm (A-D).

https://doi.org/10.1371/journal.pone.0221006.g006

leukemia (PML) body where Hipk2-mediated phosphorylation of p53 occurs [28]. The exact nature of the Hipk nuclear domains is still unresolved, and the appearance of the nuclear structures differs between endogenous proteins and following ectopic expression of Hipk. In *Drosophila*, nuclear localization of Hipk is dependent on the small ubiquitin-related modifier (SUMO) protein (Smt3) and the sumoylation-controlled balance between nuclear and cytoplasmic Hipk has been shown to regulate the JNK signaling pathway [8]. We found that overexpression of Hipk in muscle results in very large nuclear Hipk-domains having a 'rim' of strong Hipk immunoreactivity with less labelling in the core of these structures. As these structures were much larger than the Hipk domains in wild type, it is possible that they comprise regions of aggregated Hipk. The structures were confined to the nucleus, with no evidence of large cytoplasmic Hipk-positive structures. Within the nucleus the Hipk domains were extra-nucleolar and were exclusively present in the extrachromosomal regions of the nucleus.

Hipk-mediated effects on NMJ growth

To evaluate possible mechanisms of Hipk action in the nervous system and muscle, we studied the larval NMJ and found that NMJ size in Hipk over-expressing animals was significantly larger in comparison to wild-type controls. Strikingly, Hts distribution in the muscle was disrupted, which could be related, at least in part, to the NMJ growth effect. Adducin/Hts is an actin- and spectrin- binding protein that is present both pre- and post-synaptically at the larval NMJ, as well as throughout the muscle, and we have previously shown that over-expression of Hts in the muscle elevates the transcript levels of the important protein kinases CaMKII and PAR-1 in the muscle cytoplasm [20,24]. In contrast, *hts* mutants result in a loss of *camkII* and *par-1* transcripts, similar to what we observe with Hipk over-expression. Our observations that Hipk is associated with disruptions in Hts distribution in the muscle, as well as decreased transcripts and immunoreactivity of CaMKII and PAR-1, might be of functional significance. However, Hipk-mediated effects on NMJ growth most likely involve multiple inputs. In this study, we show that the levels of different synaptic proteins can either be elevated, inhibited or unaffected with Hipk over-expression, indicating a complex mode of regulation. In addition, we also provide evidence that Hipk can interact with at least one ALS-associated gene.

To further study Hipk nuclear functions, we examined two proteins involved in neurodegeneration that are expressed in fly muscle nuclei: TBPH/TDP-43 and Caz/FUS. These proteins have been studied extensively, *e.g*. both loss and gain of TDP-43 function, in addition to TDP-43 redistribution from the nucleus to the cytoplasm, is frequently observed both in the neurodegenerative disorder, ALS, and in fly models of ALS [30,36]. We evaluated TBPH levels in Hipk over-expressing larval muscle nuclei. Under these conditions, we observed a striking decrease in nuclear TBPH immunoreactivity in comparison to the wild-type control. These findings suggest that Hipk may regulate TBPH nuclear loss or clearing either directly or indirectly. In contrast, another nuclear protein involved in neurodegeneration and in familial ALS, FUS (Caz) is not affected by Hipk modulation suggesting that the effects we observe with TBPH are not simply due to nonspecific effects on nuclear proteins.

Our results are also of interest in relation to recent work showing that activation of Hipk2 promotes endoplasmic reticulum (ER) stress and neurodegeneration in an animal model of ALS [37]. The effect of Hipk2 in ALS may be mediated by TDP-43, as well as the JNK signaling pathway. Cytosolic TDP-43 is often found to be phosphorylated in tissue from ALS patients and an elevation of phosphorylated Hipk2 (at S359/T360) was found to be positively correlated with the level of ubiquitinated TDP-43 in tissue from ALS patients, post-mortem [37]. Hipk2 inhibition reduced the neurodegeneration associated with ER stress *in vitro* produced either by tunicamycin or by altered expression of wild-type or mutant TDP-43 [37]. Interestingly, mice having mutations in FUS/TLS that are associated with familial ALS did not demonstrate the altered Hipk2 levels, consistent with our observations that Hipk over-expression did not alter the distribution of nuclear Caz, or produce a rough eye phenotype with Caz over-expression. However, it is possible that given the many signaling pathways that are triggered by Hipk, other potential mechanisms for neurotoxicity exist. For instance, Hipk2 has also been linked to transcriptional control of N-methyl-D-aspartate receptors, which are well established to be involved in neuronal cell death [38].

Our data demonstrate that in addition to having roles in tumorigenesis Hipk also has profound effects on the nervous system and muscle including on the NMJ. This work also indicates that in addition to modifying phosphorylation of nuclear proteins, Hipk affects the distribution of nuclear proteins and also can influence the phosphorylation state of extranuclear proteins, either directly or indirectly affecting function and viability.

Materials and methods

Fly stocks

All stocks were maintained at 25˚C or 18˚C. The *UAS-hipk*-RNAi line (17090R-1) used for most of the current work was obtained from the National Institute of Genetics stock centre (https://shigen.nig.ac.jp/fly/nigfly/). Unless otherwise specified, *UAS-hipk*-RNAi refers to this stock. A second *UAS-hipk*-RNAi line (termed V2; 108254) used for some crosses was obtained from the VDRC stock centre. *UAS-HA-hipk* (also referred to as UAS-Hipk^{3M}) is described in [3] and attP40 *UAS-HA-hipk* described in [39]. For the purposes of this study, UAS-Hipk refers to the *UAS-Hipk^{3M}* stock, unless otherwise noted. The following lines were obtained from the Bloomington *Drosophila* Stock Center: *w^{1118}* (3605); *UAS-w*-RNAi (33762); *UAS-myr-RFP* (7118); *w*; P{tubP-Gal80ts}20; TM2/TM6B, Tb (Gal80^{ts}* on chromosome 3; 7019 *P{tubP-Gal80^{ts}}2* (*Gal80^{ts}* on chromosome 3; 7017); *y w*; *P{Gal4-Mef2.R}3 (Mef2-Gal4*; 27390); *ple-Gal4* (8848); *ChAT-Gal4.7.4-19B* (6798); *ChAT-DD. Gal4.VP16* (64410); *GawB elav^{C155}* (*elav-Gal4*; 458); *GawB V Glut^{OK371}* (26160); *GawB D42* (8816); *repo-Gal4* (7415); *w**; *P{long-GMR-Gal4}2* (*longGMR-Gal4*; *8605*); *y w*; *wg^{Sp-1}/CyO*; *P{longGMR-Gal4}3/TM2* (*long-GMR-Gal4*; 8121); *hipk-Gal4* (BG00855, 12779). The *Appl-Gal4* line was kindly provided by Dr. U. Pandey. The *UAS-TBPH* and *UAS-caz* lines were kindly provided by Dr. B. McCabe. The *TH-Gal4* line was kindly provided by Dr. D. Allan. The ey-Flp [*eyflp[122]; Act>y +>GAL4,UAS-GFP; MKRS/TM6B*] stock was provided by Dr. A. Singh. The following stocks were constructed for the adult survival experiments and analysis of eye effects: (i) *UAS-hipk*-RNAi/UAS-*hipk*-RNAi; *Gal80^{ts}/Gal80^{ts}* (ii) *Gal80^{ts}/Gal80^{ts}*; *UAS-HA-hipk/UAS-HA-hipk* (iii) *Gal80^{ts}/Gal80^{ts}*; *Tub-Gal4/TM3, Sb* (iv) *Dicer-2/Dicer-2*; *Tub-Gal4/TM3, Sb Ser*; (v) attP40 *UAS-HA-hipk/CyO; longGMR-Gal4/longGMR-Gal4*.

Fly crosses, lifespan and phenotypic analyses

For the lifespan analysis, homozygous UAS-*hipk-RNAi* or *UAS-HA-hipk* females were crossed to *Gal80^{ts}/Gal80^{ts}*; *Tub-Gal4/TM3, Sb* males. These crosses were set up at 18˚C and the parents were sub-cultured two or three times to fresh medium at three-day intervals and the progeny were allowed to develop to eclosion at 18˚C. Experimental and internal control males from these crosses were collected within 0–24 hours post-eclosion and shifted to 29˚C (10 flies/vial). Thereafter, the males were transferred to fresh medium, usually every 2 or 3 days, and the number of survivors was recorded at each transfer, in most cases until the last of the flies had died. The data were converted to percent survival and these values were plotted versus days at 29˚C. There were two trials each for knockdown and over-expression and two types of internal controls were included.

Crosses were conducted to test for possible developmental effects of Hipk knockdown or Hipk over-expression in the nervous system and muscles at 29˚C in two separate sets of experiments. In the first, most crosses involved mating *Gal4*-driver-bearing males to heterozygous females bearing either *UAS-hipk-RNAi* or *UAS-hipk* transgenes and appropriate balancer chromosomes (*CyO* or *TM3, Sb* or *TM3, Sb Ser*); the single exception involved the glial cell crosses, which used repo-*Gal4/TM3, Sb* females and *hipk*-transgene-bearing males. In the second set of experiments, most crosses involved mating females bearing either *UAS-hipk*-RNAi (V2)/CyO or attP40 *UAS-hipk* /CyO to *Gal4*-driver-bearing males; the single exception involved tests with the *Appl-Gal4* driver, for which reciprocal crosses were performed. In all cases, crosses were carried out in vials with ~four pairs of parents per vial and the crosses were sub-cultured on fresh medium twice at 3-day intervals. Wherever crosses showed lethality, approximate lethal phases were determined, and any phenotypes of survivors were also noted.

In addition, with respect to the first set of experiments, the eyes of surviving *elav-Gal4*/+; *UAS-hipk-RNAi*/+, *elav-Gal4*/+; *UAS-hipk*/+ females, as well as those of respective internal control *elav-Gal4*/+; *CyO*/+ and *elav-Gal4*/+; *TM3*, *Sb*/+ flies, were photographed.

To test for photoreceptor-specific effects of Hipk knockdown and over-expression, *UAS-hipk*-RNAi/*CyO* and *UAS-hipk*/*TM3*, *Sb* females were crossed separately to *longGMR-Gal4* (chromosome 2) males at 29˚C (four pairs of parents per vial) and the crosses were sub-cultured on fresh medium twice at three-day intervals. *UAS-hipk-RNAi*/*longGMR-Gal4* flies failed to eclose at 29˚C. After eclosion, the eyes of *longGMR-Gal4*/+; *UAS-hipk*/+ females and of internal control *CyO*/*longGMR-Gal4* and *longGMR-Gal4*/+; *TM3*, *Sb*/+ females, were photographed. Since pilot studies revealed that attP40 *UAS-hipk*/*longGMR-Gal4* flies developing at 29˚C did not exhibit an eye phenotype, we used this line to test for potential interactions involving simultaneous Hipk over-expression and over-expression of nuclear proteins of interest, Caz and TBPH. For this analysis, attP40 *UAS-HA-hipk*/*CyO*; *longGMR-Gal4*/*longGMR-Gal4* females were mated separately to homozygous *UAS-caz* and *UAS-TBPH* males at 29˚C (four pairs of parents per vial) and the crosses were sub-cultured on fresh medium twice at three-day intervals. In all cases, after eclosion the eyes of appropriate experimental and internal control flies were photographed (see Results for genotypes). In addition, the eyes of surviving *elav-Gal4*/+; *UAS-hipk-RNAi*/+ and *elav-Gal4*/+; *UAS-hipk*/+ and appropriate internal control females from the aforementioned developmental crosses, were also photographed.

Larval body wall preparation

Body wall dissections of crawling third instar larvae were performed as previously described [40]. For transgenic analysis, homozygous *UAS*-transgene-bearing males were crossed to homozygous *Gal4*-bearing virgin females ensuring that all progeny carried one copy of each. All crosses were maintained at 25˚C unless indicated otherwise.

Immunohistochemistry (IHC)

Immunostaining of body walls was performed as previously described [41]. The following primary antibodies were used: 1:100 goat anti-Hrp (Jackson ImmunoResearch– 123-005-021); 1:100 rabbit anti-Hrp (JIR– 323-065-021); 1:200 rabbit anti-Hipk [4]; 1:50 mouse anti-GluRIIA (Developmental Studies Hybridoma Bank– 8B4D2); 1:10 mouse anti-α-Spec (DSHB– 3A9); 1:2 mouse anti-Fas2 (DSHB– 1D4); 1:10 mouse anti-Hts (DSHB– 1B1); 1:100 goat anti-phospho-Add^{S662} (Santa Cruz Biotechnology–sc-12614); 1:200 mouse anti-CaMKII (Cosmo Bio–CAC-TNL-001-CAM); 1:200 rabbit anti-PAR-1[42], which was generously provided by Dr. Bingwei Lu (Stanford University); 1:200 rabbit anti-phospho-Dlg^{S797} [26], also from Dr. Lu; 1:200 rabbit anti-Caz [43], kindly given by Dr. Takahiko Tokuda (Kyoto Prefectural University); and 1:200 guinea pig anti-TBPH [44], a gift from Dr. Dale Dorsett (Saint Louis University). Fluorescent-labeled secondary antibodies from JIR and Vector Laboratories were all used at a 1:200 dilution. Stained body walls were mounted in VECTASHIELD Mounting Medium with DAPI (Vector–H-1200). Experiments and their controls were immunostained in the same tube, and thus exposed to the same treatment. Images of NMJs innervating muscles 6/7 from abdominal segment 3 were taken as merged stacks, unless otherwise stated, on either a Nikon A1R laser scanning confocal microscope with NIS-Elements software or a Zeiss LSM 880 with Airyscan, with experiments and their controls imaged under identical acquisition settings. All images were processed with Adobe Photoshop.

Fluorescent in situ hybridization (FISH)

FISH of body walls was performed as previously described [24]. cDNA clones (*Drosophila* Genomics Resource Center) IP15240 and RE47050 were used as templates to make DIG-

labeled, antisense probes against *camkII* and *par-1* transcripts, respectively. Experiments and their controls were processed in the same tube, and thus exposed to the same treatment. Body walls were mounted and imaged as described in the previous section.

Quantifications

Stacked confocal images of larval muscles 6/7 from abdominal segment 3 were used for measurements. Student's t-test was used for statistical analysis, and data was expressed as the mean ± S.E.M. NMJ size: For each NMJ, Hrp immunofluorescence signal was delineated using Photoshop tools and the size was measured as pixel surface area. The outline of muscles 6/7 was also selected with Photoshop and the pixel surface area was recorded. To normalize the NMJ size measurement, the NMJ pixel surface area was divided by the muscle pixel surface area. Muscle nuclei size: For each muscle 6/7 pair, DAPI signal was delineated using Photoshop tools and the combined size of all muscle nuclei was measured as total pixel surface area. To calculate the average nuclear size, the total pixel surface area was divided by the number of nuclei. Immunofluorescence intensity at the NMJ: Quantification of post-synaptic protein levels at the NMJ was calculated as a ratio between the immunofluorescence intensity of the protein of interest and Hrp, which was used as a control. Immunofluorescence signal at the NMJ was selected using Photoshop, and the intensity was determined by measuring the mean gray value. Puncta levels in the muscle: For quantification of *camkII*/*par-1* FISH puncta or p-Dlg IHC puncta in the muscle, confocal images were inverted and the threshold function of ImageJ was used to create binary images in which puncta were represented by black pixels and the background was eliminated. The number of extra-synaptic black pixels within a fixed area size was measured in both muscles 6 and 7.

Quantification of effectiveness of Hipk RNAi and over-expression transgenes. For quantification of Hipk over-expression, *Mef2-Gal4* was crossed to UAS-Hipk-attp40, UAS-Hipk3M, or UAS-myr-RFP. RNA was prepared from whole 3rd instar larvae. For RNAi-mediated knock-down, female EyFLP virgins [eyflp[122]; Act>y+>GAL4,UAS-GFP; MKRS/TM6B] were mated to male $dHipk^{RNAi\ V2}$, $dHipk^{RNAi\ NIG}$ and w^{RNAi} flies at 25˚C. Resulting larvae were screened at the late L3 stage for the presence of GFP in the eye-antennal discs, indicating successful induction of the flippase to allow for Actin-Gal4 to drive the expression of the UAS constructs. GFP positive eye discs were collected and stored in Qiagen Buffer RLT Plus supplemented with fresh 1% β-mercaptoethanol and stored at -20˚C until enough discs were collected for RNA isolation. RNA isolation was performed using Qiagen RNeasy Plus Mini Kit (Cat No. 74134), following the manufacturer's instructions. ABM Onescript® Plus cDNA Synthesis Kit (Cat No. G236) was used to generate cDNA from 50ng of RNA per sample using oligo dT primers. SensiFAST™ SYBR® Lo-ROX Kit (Cat No. BIO-94005) was used with an Applied Biosystems QuantStudio 3 to perform Real-Time PCR. RP49 was used as a reference gene. All samples were tested in triplicate. Error bars show Min and Max RQ values.

Supporting information

S1 Fig. qRT-PCR quantification showing efficiency of knock-down and over-expression of Hipk transgenes. *hipk* mRNA levels were quantified using qRT-PCR of tissue extracts. (A) Shows relative *hipk* expression levels following expression of w^{RNAi} (control), $dHipk^{RNAi\ V2}$ and $dHipk^{RNAi\ NIG}$ using Ey-Flp (as described in methods). (B) For quantification of Hipk over-expression, *Mef2-Gal4* was crossed to UAS-myr-RFP (control), UAS-Hipk-attp40 and UAS-Hipk3M. All samples were tested in triplicate. Error bars show Min and Max RQ values. (TIF)

S2 Fig. Hipk-mediated effects on NMJ and muscle nuclei size. From stacked confocal images of muscles 6/7, NMJs (marked by Hrp), muscle nuclei (marked by DAPI) and muscles were delineated with Photoshop selection tools and their sizes were measured as pixel surface area. (A) Hipk over-expression in the muscle (*Mef2-Gal4>hipk*) led to significantly larger NMJs (an approximately 1.2 fold increase) when compared to the wild-type control (i.e. *Mef2-Gal4* out-crossed to w^{1118}). (B-C) Hipk over-expression also resulted in a slight increase in muscle nuclei (25.9±0.7 nuclei in muscles 6 and 7 combined, in comparison to 22.2±0.5 in the wild-type control), which were significantly bigger on average (an approximately 1.5 fold increase). (D) Quantification shows that Hipk over-expressors had significantly smaller muscles (an approximately 1.2 fold decrease), indicating that the measured Hipk-mediated effects on NMJ (A) and muscle nuclei (C) size shown here are not simply due to increased muscle size. Sample size was 24 muscle 6/7 pairs from 12 body walls for each genotype. * $p = 0.0106$; ** $p < 0.0001$.
(TIF)

S3 Fig. Hipk knock-down in the muscle during larval NMJ development. (A) A typical 3rd instar larval NMJ, marked by Hrp, innervating muscles 6/7 in abdominal segment 3. (B) Muscle-specific expression of transgenic *hipk-RNAi* (*Mef2-Gal4>hipk-RNAi*) resulted in NMJ (note the slightly diffuse Hrp labeling) and muscle morphological defects. Scale bar: 40μm (A, B).
(TIF)

S4 Fig. Hipk-mediated effects on different post-synaptic proteins. Post-synaptic protein levels at the NMJ was calculated as a ratio between the immunofluorescence intensity of the protein of interest and Hrp, which was used as a staining control. Immunofluorescence signal at the NMJ was selected using Photoshop, and the intensity was determined by measuring the mean gray value. (A) No significant effects on the levels of GluRIIA at the NMJ were observed between muscle-specific Hipk over-expression and the control. n = 8 (over 4 body walls) for each genotype. (B) However, Hipk over-expression resulted in significantly lower synaptic levels of α-Spec. n = 8 (over 4 body walls) for each genotype. (D) Hipk over-expression also resulted in significantly higher Fas2 synaptic levels. n = 8 (over 4 body walls) for each genotype. *** $p < 0.0001$.
(TIF)

S5 Fig. Hipk-mediated effects on Hts and p-Add levels at the NMJ. Hts total and phosphorylation levels at the NMJ were calculated as a ratio between Hts or p-Add immunofluorescence intensity and Hrp, which was used as a staining control. Immunofluorescence signal at the NMJ was selected using Photoshop, and the intensity was determined by measuring the mean gray value. (A) Hipk over-expression in the muscle resulted in a slight, but significant, increase in Hts levels at the NMJ when compared to control. n = 8 (over 4 body walls) for each genotype. (B) In contrast, Hipk over-expression led to a significant decrease in p-Add levels at the NMJ. n = 8 (over 4 body walls) for each genotype. * $p = 0.0375$; ** $p = 0.0007$.
(TIF)

S6 Fig. Quantification of FISH and IHC puncta levels in the muscle. Confocal images were converted to binary images, where immunofluorescent puncta were represented as black pixels and the background was represented as white pixels (examples are shown). The number of extra-synaptic black pixels within a fixed area size of muscle was measured. (A) Muscle-specific Hipk over-expression led to significantly reduced levels of *camkII* FISH signal when compared to the control. n = 20 (over 5 body walls) for each genotype. (B) Similar results were observed for *par-1* FISH signal. n = 16 (over 4 body walls) for each genotype. (C) p-Dlg IHC signal in the muscle was also significantly lowered when Hipk was over-expressed in the

muscle. n = 16 (over 4 body walls) for each genotype. * p = 0.019; ** p = 0.0007; *** $p < 0.0001$. Scale bars: 40μm (A); 40μm (B); 40μm (C).
(TIF)

S7 Fig. Hipk-mediated effects on the nuclear proteins, Caz and TBPH. Muscle nuclear levels were calculated as a ratio between either Caz or TBPH immunofluorescence intensity and DAPI, which was used as a staining control. Immunofluorescence signal in muscle nuclei was selected using Photoshop, and the intensity was determined by measuring the mean gray value. (A) No significant effects on the nuclear levels of Caz were observed between muscle-specific Hipk over-expression and the control. n = 10 (over 5 body walls) for each genotype. (B) However, Hipk over-expression resulted in a significant decrease in TBPH nuclear levels when compared to the wild-type control. n = 10 (over 5 body walls) for each genotype. * p = 0.0338.
(TIF)

S1 Table. Tests for viability of *hipk* knockdown in various nervous system components and muscles using the VDRC *UAS-hipk-RNAi*.
(DOCX)

S2 Table. Tests for viability of *hipk* over-expression in various nervous system components and muscles using the attP40 *UAS-HA-hipk*.
(DOCX)

Acknowledgments

We are grateful to the Bloomington *Drosophila* Stock Center (NIH P40OD018537), Vienna *Drosophila* RNAi Center (VDRC), National Institute of Genetics (NIG), *Drosophila* Genomics Resource Center and Developmental Studies Hybridoma Bank for providing fly strains, cDNA clones and antibodies. We thank Dr. Leslie Griffith (Brandeis University) for her correspondence regarding CaMKII antibodies.

Author Contributions

Conceptualization: Simon J. H. Wang, Donald A. R. Sinclair, Charles Krieger, Nicholas Harden, Esther M. Verheyen.

Formal analysis: Simon J. H. Wang, Donald A. R. Sinclair.

Funding acquisition: Charles Krieger, Nicholas Harden, Esther M. Verheyen.

Investigation: Simon J. H. Wang, Donald A. R. Sinclair, Hae-Yoon Kim, Stephen D. Kinsey, Byoungjoo Yoo, Claire R. Y. Shih, Kenneth K. L. Wong.

Supervision: Charles Krieger, Nicholas Harden, Esther M. Verheyen.

Writing – original draft: Simon J. H. Wang, Donald A. R. Sinclair, Charles Krieger, Nicholas Harden, Esther M. Verheyen.

Writing – review & editing: Simon J. H. Wang, Donald A. R. Sinclair, Charles Krieger, Nicholas Harden, Esther M. Verheyen.

References

1. Kim YH, Choi CY, Lee SJ, Conti MA, Kim Y. Homeodomain-interacting protein kinases, a novel family of co-repressors for homeodomain transcription factors. J Biol Chem. 1998; 273: 25875–9. https://doi.org/10.1074/jbc.273.40.25875 PMID: 9748262

2. Blaquiere JA, Verheyen EM. Homeodomain-Interacting Protein Kinases: Diverse and Complex Roles in Development and Disease. Curr Top Dev Biol. 2017; 123: 73–103. https://doi.org/10.1016/bs.ctdb.2016.10.002 PMID: 28236976

3. Lee W, Andrews BC, Faust M, Walldorf U, Verheyen EM. Hipk is an essential protein that promotes Notch signal transduction in the Drosophila eye by inhbition of the global co-repressor Groucho. Dev Biol. Nov. 5, 20. 2009; 325: 263–272. https://doi.org/10.1016/j.ydbio.2008.10.029 PMID: 19013449

4. Blaquiere JA, Wong KKL, Kinsey SD, Wu J, Verheyen EM. Homeodomain-interacting protein kinase promotes tumorigenesis and metastatic cell behavior. Dis Model Mech. 2018; 11: dmm031146. https://doi.org/10.1242/dmm.031146 PMID: 29208636

5. Swarup S, Verheyen EMEM. Drosophila homeodomain-interacting protein kinase inhibits the Skp1-Cul1-F-box E3 ligase complex to dually promote Wingless and Hedgehog signaling. Proc Natl Acad Sci U S A. 2011/06/02. 2011; 108: 9887–9892. https://doi.org/10.1073/pnas.1017548108 PMID: 21628596

6. Poon CLC, Zhang X, Lin JI, Manning SA, Harvey KF. Homeodomain-interacting protein kinase regulates Hippo pathway-dependent tissue growth. Curr Biol. 2012; 22: 1587–94. https://doi.org/10.1016/j.cub.2012.06.075 PMID: 22840515

7. Chen J, Verheyen EM. Homeodomain-Interacting Protein Kinase Regulates Yorkie Activity to Promote Tissue Growth. Curr Biol. 2012/07/31. 2012; 22: 1582–1586. https://doi.org/10.1016/j.cub.2012.06.074 PMID: 22840522

8. Huang H, Du G, Chen H, Liang X, Li C, Zhu N, et al. Drosophila Smt3 negatively regulates JNK signaling through sequestering Hipk in the nucleus. Development. 2011/05/13. 2011; 138: 2477–2485. https://doi.org/10.1242/dev.061770 PMID: 21561986

9. Berber S, Wood M, Llamosas E, Thaivalappil P, Lee K, Liao BM, et al. Homeodomain-Interacting Protein Kinase (HPK-1) regulates stress responses and ageing in C. elegans. Sci Rep. 2016; 6: 19582. https://doi.org/10.1038/srep19582 PMID: 26791749

10. Blaquiere JA, Lee W, Verheyen EM. Hipk promotes photoreceptor differentiation through the repression of Twin of eyeless and Eyeless expression. Dev Biol. 2014; 390: 14–25. https://doi.org/10.1016/j.ydbio.2014.02.024 PMID: 24631217

11. Lee W, Andrews BC, Faust M, Walldorf U, Verheyen EM. Hipk is an essential protein that promotes Notch signal transduction in the Drosophila eye by inhbition of the global co-repressor Groucho. Dev Biol. Nov. 5, 20. 2009; 325: 263–272. https://doi.org/10.1016/j.ydbio.2008.10.029 PMID: 19013449

12. Aikawa Y, Nguyen LA, Isono K, Takakura N, Tagata Y, Schmitz ML, et al. Roles of HIPK1 and HIPK2 in AML1- and p300-dependent transcription, hematopoiesis and blood vessel formation. EMBO J. 2006; 25: 3955–3965. https://doi.org/10.1038/sj.emboj.7601273 PMID: 16917507

13. Inoue T, Kagawa T, Inoue-Mochita M, Isono K, Ohtsu N, Nobuhisa I, et al. Involvement of the Hipk family in regulation of eyeball size, lens formation and retinal morphogenesis. FEBS Lett. 2010; 584: 3233–3238. https://doi.org/10.1016/j.febslet.2010.06.020 PMID: 20579985

14. Isono K, Nemoto K, Li Y, Takada Y, Suzuki R, Katsuki M, et al. Overlapping roles for homeodomain-interacting protein kinases hipk1 and hipk2 in the mediation of cell growth in response to morphogenetic and genotoxic signals. Mol Cell Biol. 2006; 26: 2758–2771. https://doi.org/10.1128/MCB.26.7.2758-2771.2006 PMID: 16537918

15. Doxakis E, Huang EJ, Davies AM. Homeodomain-interacting protein kinase-2 regulates apoptosis in developing sensory and sympathetic neurons. Curr Biol. 2004; 14: 1761–1765. https://doi.org/10.1016/j.cub.2004.09.050 PMID: 15458648

16. Wiggins AK, Wei G, Doxakis E, Wong C, Tang AA, Zang K, et al. Interaction of Brn3a and HIPK2 mediates transcriptional repression of sensory neuron survival. J Cell Biol. 2004; 167: 257–267. https://doi.org/10.1083/jcb.200406131 PMID: 15492043

17. Zhang J, Pho V, Bonasera SJ, Holtzman J, Tang AT, Hellmuth J, et al. Essential function of HIPK2 in TGFbeta-dependent survival of midbrain dopamine neurons. Nat Neurosci. 2007; 10: 77–86. https://doi.org/10.1038/nn1816 PMID: 17159989

18. Thurmond J, Goodman JL, Strelets VB, Attrill H, Gramates LS, Marygold SJ, et al. FlyBase 2.0: The next generation. Nucleic Acids Res. 2019; 47: D759–D765. https://doi.org/10.1093/nar/gky1003 PMID: 30364959

19. Pielage J, Bulat V, Zuchero JB, Fetter RD, Davis GW. Hts/Adducin controls synaptic elaboration and elimination. Neuron. 2011; 69: 1114–31. https://doi.org/10.1016/j.neuron.2011.02.007 PMID: 21435557

20. Wang S, Sanny J, Lee J, Dong K, Harden N, Yang J, et al. Drosophila adducin regulates Dlg phosphorylation and targeting of Dlg to the synapse and epithelial membrane. Dev Biol. 2011; 357: 392–403. https://doi.org/10.1016/j.ydbio.2011.07.010 PMID: 21791202

21. Han B, Zhou R, Xia C, Zhuang X. Structural organization of the actin-spectrin-based membrane skeleton in dendrites and soma of neurons. Proc Natl Acad Sci U S A. 2017; 114: E6678–E6685. https://doi.org/10.1073/pnas.1705043114 PMID: 28739933

22. Xu K, Zhong G, Zhuang X. Actin, Spectrin, and Associated Proteins Form a Periodic Cytoskeletal Structure in Axons. Science (80-). 2013; 339: 452–456. https://doi.org/10.1126/science.1232251 PMID: 23239625

23. Matsuoka Y, Li X, Bennett V. Adducin Is an In Vivo Substrate for Protein Kinase C: Phosphorylation in the MARCKS-related Domain Inhibits Activity in Promoting Spectrin–Actin Complexes and Occurs in Many Cells, Including Dendritic Spines of Neurons. J Cell Biol. 1998; 142: 485–497. https://doi.org/10.1083/jcb.142.2.485 PMID: 9679146

24. Wang S, Tsai A, Wang M, Yoo S, Kim H -y, Yoo B, et al. Phospho-regulated Drosophila adducin is a determinant of synaptic plasticity in a complex with Dlg and PIP2 at the larval neuromuscular junction. Biol Open. 2014; 3: 1196–1206. https://doi.org/10.1242/bio.20148342 PMID: 25416060

25. Koh YH, Popova E, Thomas U, Griffith LC, Budnik V. Regulation of DLG localization at synapses by CaMKII-dependent phosphorylation. Cell. 1999; 98: 353–63. https://doi.org/10.1016/s0092-8674(00)81964-9 PMID: 10458610

26. Zhang Y, Guo H, Kwan H, Wang J-W, Kosek J, Lu B. PAR-1 Kinase Phosphorylates Dlg and Regulates Its Postsynaptic Targeting at the Drosophila Neuromuscular Junction. Neuron. 2007; 53: 201–215. https://doi.org/10.1016/j.neuron.2006.12.016 PMID: 17224403

27. Krieger C, Wang S, Yoo SH, Harden N. Adducin at the Neuromuscular Junction in Amyotrophic Lateral Sclerosis: Hanging on for Dear Life. Front Cell Neurosci. 2016; 10: https://doi.org/10.3389/fncel.2016.00011 PMID: 26858605

28. Moller A, Sirma H, Hofmann TG, Rueffer S, Klimczak E, Droge W, et al. PML is required for homeodomain-interacting protein kinase 2 (HIPK2)-mediated p53 phosphorylation and cell cycle arrest but is dispensable for the formation of HIPK domains. Cancer Res. 2003; 63: 4310–4314. PMID: 12907596

29. Rinaldo C, Siepi F, Prodosmo A, Soddu S. HIPKs: Jack of all trades in basic nuclear activities. Biochimica et Biophysica Acta—Molecular Cell Research. 2008. pp. 2124–2129. https://doi.org/10.1016/j.bbamcr.2008.06.006 PMID: 18606197

30. Casci I, Pandey UB. A fruitful endeavor: Modeling ALS in the fruit fly. Brain Res. 2015; 1607: 47–74. https://doi.org/10.1016/j.brainres.2014.09.064 PMID: 25289585

31. Buratti E, Baralle FE. Characterization and Functional Implications of the RNA Binding Properties of Nuclear Factor TDP-43, a Novel Splicing Regulator of *CFTR* Exon 9. J Biol Chem. 2001; 276: 36337–36343. https://doi.org/10.1074/jbc.M104236200 PMID: 11470789

32. Lanson NA, Maltare A, King H, Smith R, Kim JH, Taylor JP, et al. A Drosophila model of FUS-related neurodegeneration reveals genetic interaction between FUS and TDP-43. Hum Mol Genet. 2011; 20: 2510–2523. https://doi.org/10.1093/hmg/ddr150 PMID: 21487023

33. Chou C-C, Zhang Y, Umoh ME, Vaughan SW, Lorenzini I, Liu F, et al. TDP-43 pathology disrupts nuclear pore complexes and nucleocytoplasmic transport in ALS/FTD. Nat Neurosci. 2018; 21: 228–239. https://doi.org/10.1038/s41593-017-0047-3 PMID: 29311743

34. Lee W, Swarup S, Chen J, Ishitani T, Verheyen EM. Homeodomain-interacting protein kinases (Hipks) promote Wnt/Wg signaling through stabilization of beta-catenin/Arm and stimulation of target gene expression. Development. 2008/12/18. 2009; 136: 241–251. https://doi.org/10.1242/dev.025460 PMID: 19088090

35. Chalazonitis A, Tang A a, Shang Y, Pham TD, Hsieh I, Setlik W, et al. Homeodomain interacting protein kinase 2 regulates postnatal development of enteric dopaminergic neurons and glia via BMP signaling. J Neurosci. 2011; 31: 13746–57. https://doi.org/10.1523/JNEUROSCI.1078-11.2011 PMID: 21957238

36. Chang J-C, Morton DB. Drosophila lines with mutant and wild type human TDP-43 replacing the endogenous gene reveals phosphorylation and ubiquitination in mutant lines in the absence of viability or lifespan defects. Pandey U, editor. PLoS One. 2017; 12: e0180828. https://doi.org/10.1371/journal.pone.0180828 PMID: 28686708

37. Lee S, Shang Y, Redmond SA, Urisman A, Tang AA, Li KH, et al. Activation of HIPK2 Promotes ER Stress-Mediated Neurodegeneration in Amyotrophic Lateral Sclerosis. Neuron. 2016; 91: 41–55. https://doi.org/10.1016/j.neuron.2016.05.021 PMID: 27321923

38. Shang Y, Zhang J, Huang EJ. HIPK2-Mediated Transcriptional Control of NMDA Receptor Subunit Expression Regulates Neuronal Survival and Cell Death. J Neurosci. 2018; 38: 4006–4019. https://doi.org/10.1523/JNEUROSCI.3577-17.2018 PMID: 29581378

39. Tettweiler G, Blaquiere JA, Wray NB, Verheyen EM. Hipk is required for JAK/STAT signal transduction during development and tumorigenesis. PLoS One. 2019; 14(12): e0226856. https://doi.org/10.1371/journal.pone.0226856 PMID: 31891940

40. Wang S, Yoo S, Kim H, Wang M, Zheng C, Parkhouse W, et al. Detection of In Situ Protein-protein Complexes at the Drosophila Larval Neuromuscular Junction Using Proximity Ligation Assay. J Vis Exp. 2015; 95: 52139. https://doi.org/10.3791/52139 PMID: 25650626

41. Ramachandran P, Budnik V. Immunocytochemical Staining of *Drosophila* Larval Body-Wall Muscles. Cold Spring Harb Protoc. 2010; 2010: pdb.prot5470. https://doi.org/10.1101/pdb.prot5470 PMID: 20679379

42. Sun TQ, Lu B, Feng JJ, Reinhard C, Jan YN, Fantl WJ, et al. PAR-1 is a Dishevelled-associated kinase and a positive regulator of Wnt signalling. Nat Cell Biol. 2001; 3: 628–636. https://doi.org/10.1038/35083016 PMID: 11433294

43. Sasayama H, Shimamura M, Tokuda T, Azuma Y, Yoshida T, Mizuno T, et al. Knockdown of the Drosophila fused in sarcoma (FUS) homologue causes deficient locomotive behavior and shortening of motoneuron terminal branches. Iijima KM, editor. PLoS One. 2012; 7: e39483. https://doi.org/10.1371/journal.pone.0039483 PMID: 22724023

44. Swain A, Misulovin Z, Pherson M, Gause M, Mihindukulasuriya K, Rickels RA, et al. Drosophila TDP-43 RNA-Binding Protein Facilitates Association of Sister Chromatid Cohesion Proteins with Genes, Enhancers and Polycomb Response Elements. PLoS Genet. 2016; 12: e1006331. https://doi.org/10.1371/journal.pgen.1006331 PMID: 27662615